New Journal of Physics
The open access journal for physics

Flux pattern transitions in the intermediate state of a type-I superconductor driven by an ac field

J Ge[1], J Gutierrez, B Raes, J Cuppens and V V Moshchalkov
INPAC—Institute for Nanoscale Physics and Chemistry, KU Leuven, Celestijnenlaan 200D, B-3001 Leuven, Belgium
E-mail: Junyi.Ge@fys.kuleuven.be

New Journal of Physics **15** (2013) 033013 (12pp)
Received 7 December 2012
Published 12 March 2013
Online at http://www.njp.org/
doi:10.1088/1367-2630/15/3/033013

Abstract. The intermediate state of a type-I superconductor Pb film is studied by a scanning Hall probe and scanning ac-susceptibility microscopies under static and oscillating applied magnetic fields. The structure of the typical flux patterns during magnetic field penetration/expulsion shows a strong hysteresis. Under the action of an ac field, the multiply quantized flux tubes in a type-I superconductor reveal a dynamical reordering similar to what is observed in the Campbell regime for vortices in a type-II superconductor. Most strikingly, after shaking, higher density flux tube patterns demonstrate a reorganization from a superheated metastable tubular pattern to a stable stripe pattern. We provide direct experimental evidence that the flux reorganization behavior is a dynamical transition. The local distribution of the potentials providing pinning to intermediate state patterns is mapped out, which is, as far as we know, the first direct visualization of confinement of intermediate state domains by pinning centers.

S Online supplementary data available from stacks.iop.org/NJP/15/033013/mmedia

[1] Author to whom any correspondence should be addressed.

Contents

1. Introduction

Over the last few years, driven elastic media in the presence of quenched disorder have often been found to show a self-reorganization into a more equilibrium and ordered state [1–6]. One of the most extensively studied systems is the driven vortex lattice (VL) in type-II superconductors with random pinning. It has been found that under a dc-driven force, e.g. by applying a dc flow current, there are three dynamical phases for the vortex matter [7] and at high drives the disordered lattice in the plastic flow regime undergoes a striking dynamical transition into an ordered state [8]. Moreover, an oscillating drive is found to lead to new experimental observations which cannot be explained by the force-dependent evolution of a steadily driven VL. Both numerical simulations [1] and experimental studies [9, 10] have demonstrated that an oscillating drive can assist the VL ordering even when the vortices are plastic if the same force is applied in a constant way, indicating that oscillatory dynamics plays an essential role.

Besides the systems with triangular lattices, numerical studies [11] have indicated that such dynamical phases and reordering transitions may also occur in systems with competing short- and long-range interactions such as the intermediate state (IS) of type-I superconductors, ferrofluids, amphiphilic monolayers, adsorbates on a metal substrate [12]. In type-I superconducting samples with a geometry that promotes demagnetizing effects, the competition arises from the positive surface energy between the normal (N) and superconducting (S) domains which favors short-range attraction, and the magnetic energy which results in the long-range repulsions [13–15]. Compared with the aforementioned systems, the accessibility of the IS and the possibility of manipulation of its thermodynamical parameters make type-I superconductors a very convenient model system to gain a deeper insight into the physics of ac-shaking-induced transitions between different IS patterns.

So far, there have been only a few reports on the dc-driven transformation of the IS. By applying a high driving current, Hoberg and Prozorov [16] observed the transition from laminar structure to tubular pattern, suggesting that tubular pattern represents the most equilibrium state. It has also been found that stripe patterns can undergo a restructuring to tubes after cycling the magnetic field periodically [17]. However, a theoretical estimate made by Goren and Tinkham [13] showed that the tubular and the laminar patterns have approximately the same energy. This means that the equilibrium superconducting state in IS can be easily affected by various factors such as the presence of pinning centers and differences in sample geometry. Magneto-optical studies revealed that the differences in flux structures (topological hysteresis)

can even lead to a residual magnetic hysteresis in the most carefully prepared defect-free samples [18]. Therefore, the dynamical response of the IS under an oscillating drive can be very complex. Studying this phenomenon would shed light on the relationship between flux patterns, the equilibrium state and the interactions between them and the pinning centers in the IS.

In this paper, we have studied the flux configurations and dynamical behaviors of the IS of a type-I lead film with a substantial amount of intrinsic pinning centers by using the combined high-resolution scanning Hall probe microscopy (SHPM) and scanning ac-susceptibility microscopy (SSM) [19] techniques. At low flux densities and driving forces, we found a similar dynamical behavior between the flux tubes in the IS and the vortices in the mixed state in a type-II superconductor under the influence of disorder. For high flux densities, however, a gentle ac drive is sufficient to restructure the flux from a tubular to a stripe pattern. The distribution of pinning centers is mapped out by two different approaches. We demonstrate the strong influence of pinning on the structure of the visualized flux patterns, and the dynamical behavior of different flux configurations.

2. Experimental details

The investigated sample is a thick lead film with a lateral dimension of $1 \times 1\,\mathrm{cm}^2$ and a thickness of $d = 5\,\mu\mathrm{m}$. The sample was grown using an e-beam evaporation system. A 10 nm Ge layer was deposited on top to protect the Pb surface from oxidation. There is no obvious difference among the edges of the sample; therefore, the penetration of the flux is considered to be the same. The superconducting critical temperature is $T_c = 7.05\,\mathrm{K}$, as determined by the ac susceptibility at zero applied magnetic field. The SHPM images were obtained using a modified low-temperature scanning Hall probe microscope from Nanomagnetics Instruments with a temperature stability better than 1 mK and a magnetic field resolution of 0.1 G [19–22]. The chosen location for the SHPM experiments is close to the center of the film, and the scanned area covers a surface of $16 \times 16\,\mu\mathrm{m}^2$. Different areas of the sample, within $100\,\mu\mathrm{m}$ distance of each other, have been investigated. The results are similar, which leads to very consistent conclusions. The images are recorded in 'lift-off' mode by moving the Hall cross above the sample surface at a height of $\sim 1\,\mu\mathrm{m}$. All the experiments have been performed with the field applied perpendicular to the sample surface. For the SSM measurements, an ac field with a frequency $f = 25.123\,\mathrm{Hz}$ and parallel to the dc field is always used.

In this work, we have studied the flux configurations of the IS obtained by using two different modes of the flux pattern formation. Flux patterns formed during magnetic field penetration into the sample were imaged upon sweeping up the magnetic field after the sample was cooled down ($T < T_c$) in zero magnetic field. Additionally, flux patterns formed during magnetic field expulsion were investigated while sweeping down the magnetic field, after the sample was field cooled to a given fixed temperature close to $T_c(H)$.

3. Flux patterns of the intermediate state

Over the years, the origin of specific flux patterns of the IS of type-I superconductors has been a topic of long debate. In this section, we give an overview of the typical flux patterns in our Pb film in static magnetic field before studying its dynamics.

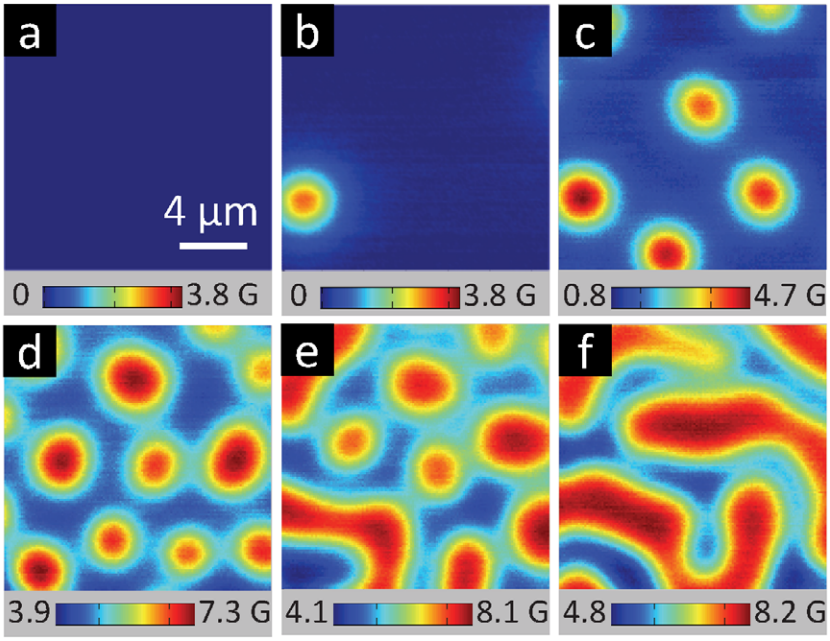

Figure 1. Typical SHPM images of type-I lead film obtained at different increasing magnetic fields after zero-field cooling (ZFC) at 6.9 K: (a) 2 Oe, (b) 2.6 Oe, (c) 4.2 Oe, (d) 7.6 Oe, (e) 12 Oe and (f) 16 Oe. Blue and red areas correspond to superconducting and normal state, respectively.

Figures 1(a)–(f) show the flux patterns of the IS obtained with the SHPM during flux penetration at 6.9 K. At low fields, the sample is in the Meissner state with no flux observed in the scanning area (figure 1(a)). When a certain magnetic field (≈2 Oe at 6.9 K) is reached, magnetic flux begins to penetrate into the sample, forming flux tubes with a rounded shape (figure 1(b)). At first, entering flux tubes have similar radii and vorticity as depicted in figure 1(c); but with further increasing the field, the density of flux tubes increases and the tubes start to lose the rounded shape characteristic of lower densities. The tubes also exhibit a broader distribution of sizes and vorticities as shown in figure 1(d). When the magnetic field reaches a certain threshold (≈12 Oe at 6.9 K), the tubes become very close to each other, the N/S positive surface energy takes over and flux tubes start to merge to form stripe-like normal domains, resulting in a state with coexistence of flux tubes and stripes (figure 1(e)). As shown in figure 1(f), once it becomes favorable for the system to form stripes, they thrive as the magnetic field increases, resulting in the formation of longer stripes, which eventually merge to form wider normal domains that cover the whole superconductor upon reaching $H_c(T)$ (≈25 Oe at 6.9 K).

Figures 2(a)–(d) show the flux patterns of the IS obtained with the SHPM during flux expulsion at 6.9 K. Figure 2(a) presents a SHPM image taken at 20 Oe and 6.9 K close to H_c; normal regions surround small superconducting regions. As we decrease the magnetic field, in contrast to the case of flux penetration, the stripe-like normal domains nucleate first (figure 2(b)) and they last to significantly lower fields (figure 2(c)), as compared with the flux penetration experiment (figure 1(e)). As we keep on decreasing the magnetic field, part of the stripes breaks down into flux tubes until only flux tubes remain (figure 2(d)). Finally, figure 2(e) shows the

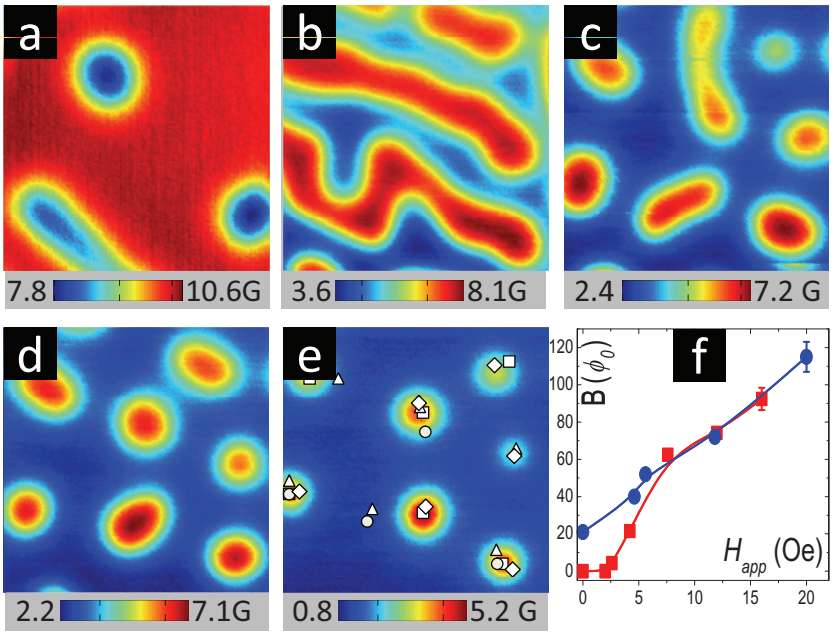

Figure 2. SHPM images measured at 6.9 K after field cooling (FC) and then progressively decrease field from (a) 20 Oe to (b) 11.8 Oe, (c) 5.6 Oe, (d) 4.6 Oe and (e) remnant field. The symbols in (e) show the positions of flux tubes after various FC processes at $T = 6.9$ K and $H = 1.1$ Oe (circles); 1.9 Oe (triangles); 4.9 Oe (squares); 5.4 Oe (diamonds). Blue and red areas correspond to superconducting and normal state, respectively. (f) Local induction B as a function of the applied magnetic field $H_{\rm app}$ for images in figures 1(a)–(f) (squares) and figures 2(a)–(e) (circles).

flux pattern when the magnetic field has been decreased to zero; it is worth noting that, due to the pinning present in our sample, we do not recover the Meissner state.

Figure 2(f) shows the hysteresis in local induction B as a function of the applied magnetic field $H_{\rm app}$ for images in figures 1(a)–(f) (squares) and figures 2(a)–(e) (circles). It is clear that, for flux penetration, even at $62.5\Phi_0$ (figure 1(d)), flux patterns remain in tubular state. However, for flux expulsion, the flux patterns change from stripe to tubular state for a magnetic flux value around $52\Phi_0$ (figure 2(c)). This supports the existence of the so-called 'topological hysteresis' in our sample [23], which has been reported previously for most of the type-I materials with the presence of pinning or geometrical barriers. In this regard, our sample is a thick film of type-I lead superconductor; therefore surface barriers and/or intrinsic pinning centers (arising due to sample growing conditions) should play an important role. In order to identify the most relevant pinning centers, we have performed at the same sample area a series of repeated FC processes at various fields and temperatures. We have observed that each time the flux tubes do nucleate around the same areas (we have labeled such areas in figure 2(e)); therefore these positions should contain dominant pinning centers which could be caused by defects in the film formed during sample growth.

A detailed H–T flux phase diagram in one scanning area is constructed by both flux penetration and expulsion processes as discussed in the supplementary material (available from

stacks.iop.org/NJP/15/033013/mmedia). Also, we noted that when sweeping up the magnetic field after a ZFC, there exists a crossover field, below which the low density flux tube patterns (LDFTP) are highly metastable, with flux tubes creeping inside the sample even after two hours' waiting (see figure s1 in the supplementary material). However, for higher densities of flux tube patterns (HDFTP) with the field above the crossover field, we found that the tubular patterns stabilize in merely a few seconds after applying the field. This difference arises probably due to the difference in magnetic flux gradient inside the sample. On the other hand, FC flux patterns are always stable since they initially nucleate in energetically preferred pinning potentials. As a result, in FC experiments we did not observe any change in the vortex configuration with time. These different behaviors observed in the stability of the flux patterns hint at a diversity of dynamical responses for the different flux states and magnetic history of the system.

4. Flux dynamics in a type-I film

To study the stability and dynamics of vortex states, many different setups have been used before, for example magnetic force microscopy [24], scanning superconducting quantum interference device microscopy [25] and SSM [19, 21, 26]. Compared with other techniques, the ac-susceptibility technique has the advantage of measuring the vortex dynamics at a higher flux density in a relative large area. By applying an ac field with various amplitudes, the SSM allows us to shake the flux lines periodically by the Lorentz force raised by the induced currents, while at the same time we can directly image the equilibrium flux patterns and record locally the in-phase and out-of-phase of the magnetic response.

Figure 3(a) shows the SHPM images of an LDFTP taken at $H = 6$ Oe after performing a ZFC down to 6.9 K. The initial flux pattern (figure 3(a)) is metastable, and the position of flux tubes keep on evolving over time (up to 2 h) as mentioned before. When applying an ac field of $h_{ac} = 0.5$ Oe and $f = 25.123$ Hz, the pattern changes (figure 3(b)I) to incorporate a new flux distribution where tubes oscillate around their new defined equilibrium positions (marked as dots in figure 3(b)I and II). Figure 3(b)II shows the in-phase SSM image; it is clearly seen that around each equilibrium position a red (to the left of the equilibrium position) and a blue (to the right of the equilibrium position) signal is observed. Where a red signal appears it means that a flux tube has moved into that spot upon increasing h_{ac}, while where a blue signal appears it means that a flux tube has moved out of that position upon increasing h_{ac}. It is expected that the more the flux tube is displaced from its equilibrium position the more intense is the in-phase signal.

The resulting oscillatory movement (depicted by the arrows) bears a close resemblance to the Campbell oscillatory behavior of a VL in the mixed state of a type-II superconductor [21]. After switching the ac field off, the vortex pattern freezes in the new equilibrium position, shown by figure 3(b)I, which, in turn, does not demonstrate any variation over time or even when applying further shaking with $h_{ac} = 0.5$ Oe. Only when a higher h_{ac} or H_{dc} is applied do the flux tubes have enough energy to overcome their pinning potentials. A similar response was first observed by Goren and Tinkham [13] when applying a driving current through a stripe of a type-I superconducting indium film. Note that by superimposing an ac field to the LDFTP, the flux tubes gain enough mobility to quickly reach an equilibrium position which otherwise takes a long time to reach. The increase in mobility observed due to the superposition of an ac field has been previously reported for a type-I superconductor [27] and has a strong similarity to the mixed state of a type-II superconductor under the action of an ac field [1].

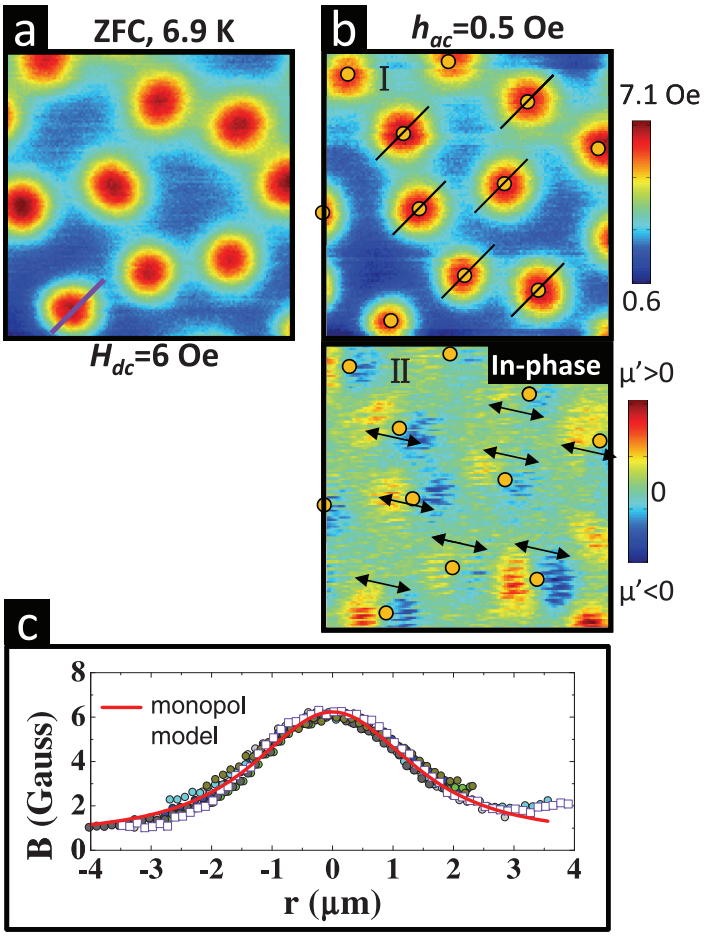

Figure 3. (a) SHPM image measured at $H = 6$ Oe after ZFC to 6.9 K. (b)I to (b)II show dc and in-phase images taken at $H = 6$ Oe and $h_{ac} = 0.5$ Oe. Dots indicate the average position of flux tubes in (b)I. The arrows show the oscillating direction of the flux tubes. (c) Cross sections (symbols) of the flux tubes as indicated by the lines in (a) and (b)I. The red line is the fit of the data of cross sections using a monopole model.

Typically, in type-II superconductors, each vortex carries only one flux quantum [28] and they experience a repulsive vortex–vortex interaction, while, on the other hand, the flux tubes in a type-I superconductor are composed of a multiple integer number of flux quanta and they demonstrate a short-range attractive interaction and a long-range weak repulsive interaction. Hence, it is natural to expect different dynamics in these systems. However, in the LDFTP, we obtained a similar dynamical behavior between flux tubes and vortices in the mixed state of type-II superconductors, where the vortices oscillate around their pinning potentials under a gentle ac field and jump from one to another at high enough ac fields [21]. Also, we noticed that the flux tubes in the LDFTP have similar diameters R, and the cross sections of the flux tubes overlap within the experimental error (figure 3(c)). The best fit of the cross sections using a monopole model [29, 30] gives a vorticity of $L \approx 6.6 \pm 1.4\Phi_0$ for each flux tube. The details of the fitting process will be published elsewhere. This indicates that all flux tubes contain a

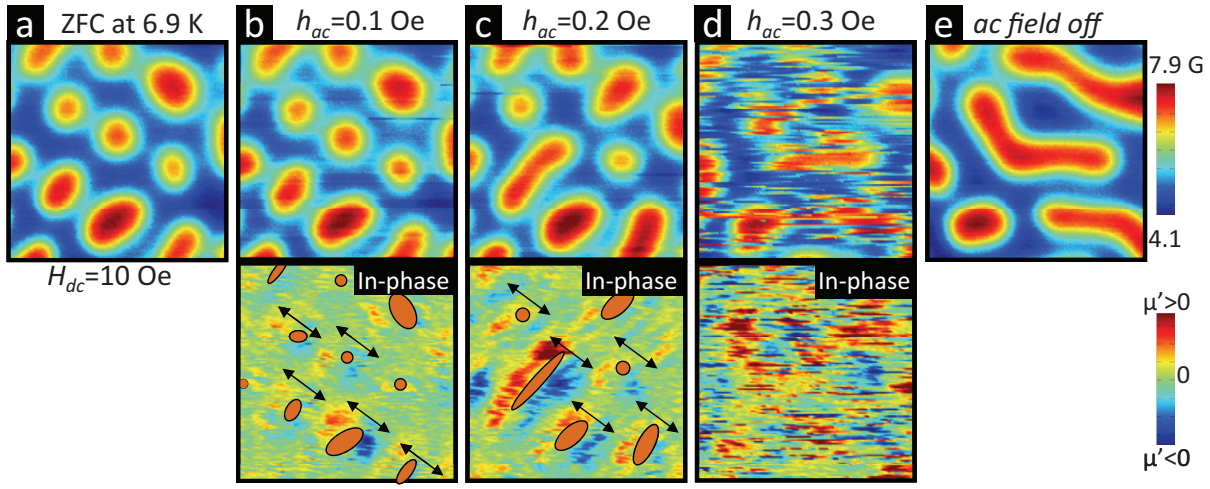

Figure 4. (a) High density flux tube state obtained at $H_{dc} = 10$ Oe after ZFC to 6.9 K. SHPM (upper panel) and SSM (lower panel) images obtained at various oscillating fields: (b) $h_{ac} = 0.1$ Oe, (c) $h_{ac} = 0.2$ Oe, (d) $h_{ac} = 0.3$ Oe; the arrows show the oscillating direction of the flux tubes. (e) SHPM image taken after switching off the ac field.

similar number of flux quanta, suggesting that the initial change of the observed tubular pattern (figure 3(b)) is not due to the split of the original flux tubes but rather due to the rearrangement of the flux lattice. Moreover, as we will later further discuss, we argue that the increase in stability of the resulting tubular patterns that occurs after applying the ac field is the result of a dynamical process which allows the flux tubes to be trapped by the randomly located pinning centers.

To further study the dynamics of the IS, we performed the experiments at a higher density of the flux tube state; figure 4(a) shows a pattern of flux tubes in such a region. If we apply a small enough h_{ac} the in-phase SSM image (figure 4(b), down panel) shows that the flux oscillates around their equilibrium positions (marked by dots and shown in the SHPM image of figure 4(b), upper panel). It should be noted that here the flux tubes are inhomogeneous in size (and magnetic field) and some are not rounded but present in an elliptical shape; still their dynamical behavior under a gentle ac-shake is similar to that obtained in the LDFTP. Nevertheless, in the HDFTP the h_{ac} needed to set the flux into motion is lower than that in the LDFTP due to the stronger interaction among the flux tubes which adapts the whole flux pattern better to available pinning centers. We can, therefore, suggest that the increase in interaction between flux tubes is the origin of the stability observed in the HDFTP during the flux penetration experiments. A similar effect was also reported in the peak effect regime of type-II superconductors which is ascribed to the collective pinning due to the softening of the elastic moduli of the VL [31].

By increasing the ac field, the vortex pattern starts to change, part of the flux tubes recombine and then they stabilize again (figure 4(c)), indicating that the 'dither force' is still not strong enough to totally overcome collective interactions. When further increasing the 'dither force' up to a critical value ($h_{ac} = 0.3$ Oe for this dc field and temperature), the dragging force applied to the flux tubes overcomes the equilibrium interaction among them and the flux tubes move by splitting and recombining together as shown in figure 4(d).

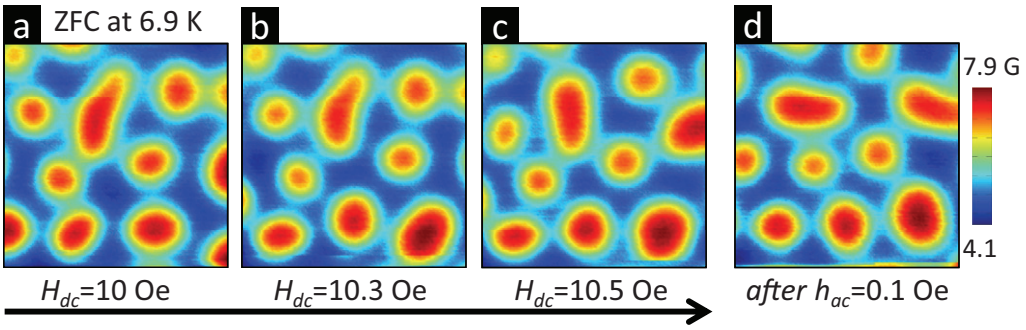

Figure 5. (a) Randomly nucleated giant vortices at 6.9 K after ZFC and then progressively increasing the magnetic field to (b) 10.3 Oe and (c) 10.5 Oe. (d) SHPM image taken after shaking the vortex pattern of (c) with $h_{ac} = 0.1$ Oe for 30 s.

After switching the ac field off, the vortex pattern has reconfigured into a coexistence state of stripes and flux tubes (figure 4(e)). To verify that the observed flux pattern reconfiguration results from a dynamical effect and not because of the increasing of the flux on applying the ac field ($H_{dc} + h_{ac}$), we measured the SHPM images at 6.9 K after ZFC and then progressively increasing the external field from 10 to 10.5 Oe (shown in figures 5(a)–(c)). Only minor changes in the vortex patterns are observed even at 10.5 Oe, thus supporting the suggestion that the reorganization of flux observed on applying an ac field in the HDFTP reflects an intrinsic dynamical behavior.

This looks quite natural because the tubular flux pattern is constrained by the collective pinning to a number of metastable states which may have a higher free energy than the equilibrium state. Since the free energy difference between the tubular state and the stripe state is quite small [16], after increasing the static field the tubular pattern has enough time to adapt to another metastable tubular state in order to compensate for the energy increase due to the increased field (a superheated tubular state). However, when applying an ac field, the tubular pattern cannot follow the rate of change of the magnetic field, i.e. before it reaches another metastable tubular pattern, the field changes again. Then all the patterns are gradually pushed into a state with a much higher energy which is unstable. After switching the ac field off, all the flux domains reorganize down to the most energy favorable state, which for this field and temperature is the stripe pattern as previously shown by the flux expulsion experiments. In figure 5(d), we show the SHPM image taken after shaking the vortex pattern of figure 5(c) (10.5 Oe) with $h_{ac} = 0.1$ Oe. Part of the flux tubes have already rearranged, which is similar to that of figure 4(c), however at a lower ac field. This is because the higher dc field ($H_{dc} = 10.5$ Oe) of figure 5(c) pushes the tubular pattern to a higher energy superheated tubular state which is less stable than that of figure 4(a); hence, a smaller dither field is needed to make the pattern change.

5. Stability of different flux states

The dynamical rearrangement of the flux domains and the FC experiments suggests that above a certain field (see figure s2 in the supplementary material, available from stacks.iop.org/NJP/15/033013/mmedia), which is temperature dependent, the stripe pattern

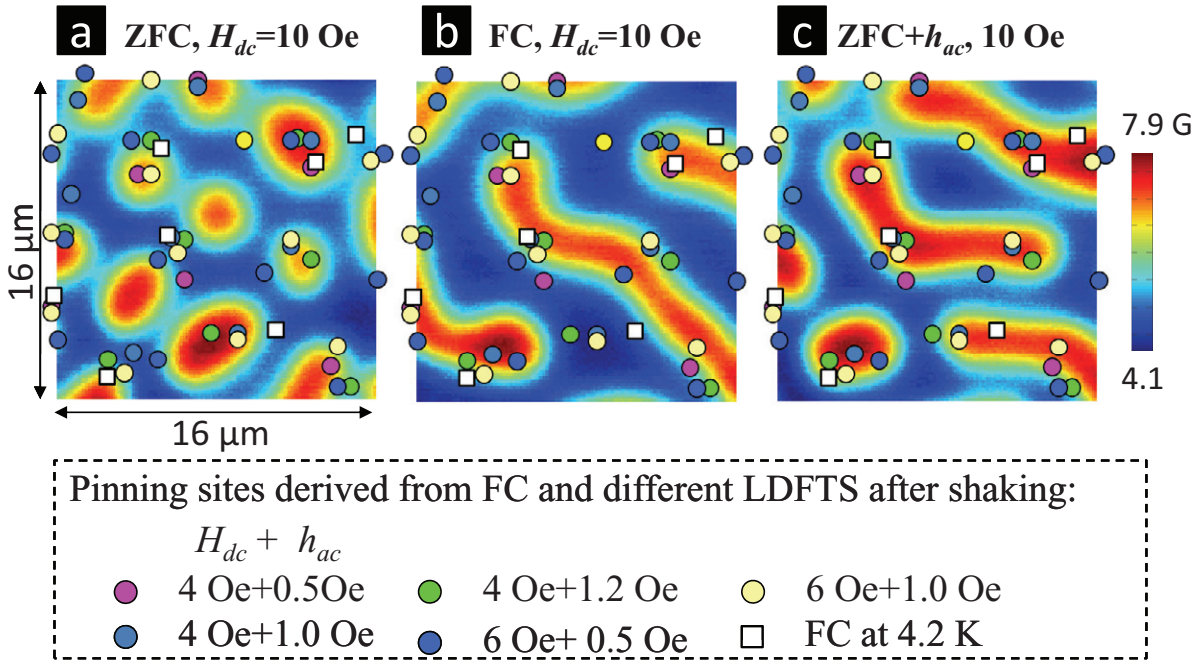

Figure 6. Vortex patterns obtained at 6.9 K with $H_{dc} = 10$ Oe after performing: (a) ZFC; (b) FC; and (c) after shaking the vortex pattern of ZFC. The dots indicate the randomly distributed pinning centers derived from the equilibrium patterns of low density flux tube state. The squares show the positions of flux tubes derived from FC at 4.2 K. ZFC and FC represent zero-field-cooling and field-cooling, respectively. LDFTS is short for low density flux tube state.

favors a low energy state compared to the flux tubes. This is totally in contrast with the case in a pinning-free sample, where the tubular pattern represents the topologically equilibrium state [16] for all magnetic fields. To unveil the mechanism behind the rearrangement of flux domains in our sample, we present in figure 6 the vortex patterns obtained at the same parameters (6.9 K, 10 Oe) after different approaches: (a) ZFC; (b) FC; (c) ZFC + h_{ac}. The intrinsic pinning potentials are also shown by the dots and the squares. The dots are derived from the equilibrium patterns of the LDFTP after shaking with various ac fields (e.g. figure 3(d)), while the squares indicate the positions of pinned flux tubes after FCs at $T = 4.2$ K. The overlap of the pinning centers, derived from different runs, further proves our claim of figure 3 that after gently shaking with an h_{ac} all the flux tubes stabilize at the pinning centers.

To further reveal the relationship between pinning centers and the magnetic flux, the following method is used: if the field value at the pinning center is bigger than 5 G, the magnetic flux is considered pinned by the pinning center, otherwise it is not. From figure 6(a), we see that the flux tubes are randomly distributed after a ZFC, with only a few of them sitting on the pinning centers (40%), which favors the picture of a superheated flux tube state stabilized by their collective interaction. However, when expelling flux out of the sample by performing field cooling, the stripe-like normal domains nucleate with 87% of pinning potentials occupied by the normal domains (figure 6(b)). This ensures a more stable state compared with that of flux penetration (figure 6(a)). Also in figure 6(c), we show the reconfigured flux tube state after shaking pattern figure 6(a) with an $h_{ac} = 0.3$ Oe as formerly discussed. It is found that 92% of

the pinning sites are well occupied by the normal domains, which shows an effect similar to the FC process. We note that performing the same experiments at different locations gives consistent results although the pinning distribution varies from scanning area to scanning area. This is reminiscent of the recent report of inverse melting on the VL in high-T_c superconductors [32], where on applying a big enough ac field, the magnetic hysteresis disappears. Therefore, we expect a reduction or even the disappearance of hysteresis in the macroscopic M–H loop with ac field on.

6. Conclusion

By using a low-temperature scanning Hall probe and scanning ac-susceptibility microscopies, we have studied the IS of a type-I superconducting lead film. By performing a series of field coolings at different temperatures and magnetic fields, we have been able to identify the positions of the strongest pinning potentials in the scanning areas of our sample. These pinning potentials could be generated by the presence of defects in the film formed during sample growth. We have found that, contrary to pinning-free samples, in our case the flux stripe pattern has a slightly lower energy than the flux tubular pattern in most of the H–T phase diagrams. Additionally, the flux tubular patterns can be further divided into two regions (LDFTP and HDFTP), which have different dynamics. Due to its metastability, the LDFTP needs a longer time (as compared to the HDFTP) to stabilize, but when subjected to a gentle ac field it reveals a dynamical rearrangement toward a stable pattern dictated by the present intrinsic pinning centers, similar to the dynamical reordering of the mixed state of a type-II superconductor under the effect of an ac-magnetic field. Contrary to the LDFTP, the HDFTP stabilizes quickly but, even for very low ac fields, it undergoes a dynamical reconfiguration to the more energy favorable flux stripe pattern. Therefore, we argue that the presence of pinning potentials plays a crucial role in determining not only the structure but also the dynamics of the IS. Moreover, in exploiting the analogies of the flux pattern dynamics in a quenched disorder of a type-I superconductor with other elastic systems with competing interactions, our new findings presented here are also important for research on dynamic phases in driven VL [9], sliding charge density [4] waves and driven Wigner crystals [33].

Acknowledgments

This work was supported by the FWO and by the Methusalem Funding from the Flemish Government.

References

[1] Valenzuela S O 2002 *Phys. Rev. Lett.* **88** 247003
[2] Pine D J, Gollub J P, Brady J F and Leshansky A M 2005 *Nature* **438** 997
[3] Nori F 1996 *Science* **271** 1373
[4] Balents L and Fisher M P A 1995 *Phys. Rev. Lett.* **75** 4270
[5] Reichhardt C and Olson C J 2002 *Phys. Rev. Lett.* **89** 078301
[6] Reichhardt C and Olson Reichhardt C J 2004 *Phys. Rev. Lett.* **93** 176405
[7] Bhattacharya S and Higgins M J 1993 *Phys. Rev. Lett.* **70** 2617
[8] Koshelev A E and Vinokur V M 1994 *Phys. Rev. Lett.* **73** 3580

[9] Henderson W, Andrei E Y and Higgins M J 1998 *Phys. Rev. Lett.* **81** 2352
[10] Paltiel Y, Zeldov E, Myasoedov Y N, Shtrikman H, Bhattacharya S, Higgins M J, Xiao Z L, Andrei E Y, Gammel P L and Bishop D J 2000 *Nature* **403** 398
[11] Reichhardt C, Reichhardt C J O, Martin I and Bishop A R 2003 *Phys. Rev. Lett.* **90** 026401
[12] Seul M and Andelman D 1995 *Science* **267** 476
[13] Goren R N and Tinkham M 1971 *J. Low Temp. Phys.* **5** 465
[14] Dorsey A T and Goldstein R E 1998 *Phys. Rev.* B **57** 3058
[15] Jeudy V, Gourdon C and Okada T 2004 *Phys. Rev. Lett.* **92** 147001
[16] Hoberg J R and Prozorov R 2008 *Phys. Rev.* B **78** 104511
[17] Menghini M and Wijngaarden R J 2007 *Phys. Rev.* B **75** 014529
[18] Prozorov R, Giannetta R W, Polyanskii A A and Perkins G K 2005 *Phys. Rev.* B **72** 212508
[19] Raes B, Van de Vondel J, Silhanek A V, de Souza Silva C C, Gutierrez J, Kramer R B G and Moshchalkov V V 2012 *Phys. Rev.* B **86** 064522
[20] Kramer R B G, Silhanek A V, Van de Vondel J, Raes B and Moshchalkov V V 2009 *Phys. Rev. Lett.* **103** 067007
[21] Kramer R B G, Ataklti G W, Moshchalkov V V and Silhanek A V 2010 *Phys. Rev.* B **81** 144508
[22] Gutierrez J, Raes B, Silhanek A V, Li L J, Zhigadlo N D, Karpinski J, Tempere J and Moshchalkov V V 2012 *Phys. Rev.* B **85** 094511
[23] Prozorov R 2007 *Phys. Rev. Lett.* **98** 257001
[24] Auslaender O M, Luan L, Straver E W J, Hoffman J E, Koshnick N C, Zeldov E, Bonn D A, Liang R, Hardy W N and Moler K A 2009 *Nature Phys.* **5** 35
[25] Kalisky B, Kirtley J R, Analytis J G, Chu J-H, Fisher I R and Moler K A 2011 *Phys. Rev.* B **83** 064511
[26] Kramer R B G, Silhanek A V, Gillijns W and Moshchalkov V V 2011 *Phys. Rev. X* **1** 021004
[27] Huebener R P 2001 *Magnetic Flux Structures in Superconductors* (Berlin: Springer)
[28] Moshchalkov V V, Baert M, Metlushko V V, Rosseel E, Van Bael M J, Temst K, Jonckheere R and Bruynseraede Y 1996 *Phys. Rev.* B **54** 7385
[29] Nishio T, Chen Q, Gillijns W, DeKeyser K, Vervaeke K and Moshchalkov V V 2008 *Phys. Rev.* B **77** 012502
[30] Wynn J C, Bonn D A, Gardner B W, Lin Y-J, Liang R, Hardy W N, Kirtley J R and Moler K A 2001 *Phys. Rev. Lett.* **87** 197002
[31] Lefebvre J, Hilke M and Altounian Z 2009 *Phys. Rev. Lett.* **102** 257002
[32] Avraham N *et al* 2001 *Nature* **411** 451
[33] Reichhardt C, Olson C J, Gronbech-Jensen N and Nori F 2001 *Phys. Rev. Lett.* **86** 4354